Journal of Alloys and Compounds 509 (2011) 6142–6145

Contents lists available at ScienceDirect

Journal of Alloys and Compounds

journal homepage: www.elsevier.com/locate/jallcom

First-principle study on electronic and structural properties of newly discovered superconductors: $CaIrSi_3$ and $CaPtSi_3$

J. Kaczkowski*, A. Jezierski

Institute of Molecular Physics, Polish Academy of Sciences, ul. M. Smoluchowskiego 17, PL-60179 Poznań, Poland

ARTICLE INFO

Article history:
Received 2 October 2010
Received in revised form 26 February 2011
Accepted 11 March 2011
Available online 21 March 2011

Keywords:
$CaIrSi_3$ and $CaPtSi_3$
Transition metal silicides
Superconductors
Density functional theory (DFT)
Electronic structure

ABSTRACT

Electronic and structural properties of newly discovered superconductors $CaIrSi_3$ and $CaPtSi_3$ were investigated using ab initio band structure methods. The crystallographic data for $CaPtSi_3$ were computed on the basis of a structural optimization method. The calculated electronic structure revealed similarities to that of the other noncentrosymmetric superconductor $BaPtSi_3$.

1. Introduction

The noncentrosymmetric superconductors have attracted attention due to their unique superconducting properties caused by the Rashba-type antisymmetric spin–orbit coupling which leads to a mixing of the spin-singlet and spin-triplet states [1]. Since the first heavy fermion noncentrosymmetric superconductor $CePt_3Si$ was discovered [2], a lot of similar systems have been found (e.g., UIr; see the review [3] and references therein). The noncentrosymmetric AMX_3 compounds (A = Ca, Ba alkaline- or Ce rare-earth metals, M = transition metal, X = Si, Ge) represent a separate class of these materials. The majority of these systems are the cerium compounds [3] which are antiferromagnetic and become superconducting only under pressure. However, a few non-cerium compounds were reported recently: $BaPtSi_3$ [4], $CaIrSi_3$ [5,6] and $CaPtSi_3$ [6] which are superconducting at ambient pressure. The superconducting transition temperatures T_c for the latter compounds take the values of 2.25 K, 3.7 K and 2.3 K, respectively. In the current paper, electronic and structural properties of $CaIrSi_3$ and $CaPtSi_3$ are calculated within the density functional framework (cf. [7] and references therein).

2. Method of calculations

The density functional calculations were done with the use of three different ab inito codes: elk-1.0.0 (FP-LAPW method) [8], Quantum-Espresso package (pseudopotentials, QE package) [9,10] and FPLO-9 [7,11,12]. The first one was used to calculate the electronic structure with and without the spin–orbit interaction (SOI). It was treated in a perturbative approach within GGA with PBE exchange-correlation functional [13]. The second code was applied to evaluate the structural parameters of both compounds. Band calculations using the full-potential relativistic local-orbital (FPLO-9) method within the local-density approximation (LDA) [14,15] have also been performed. The exchange correlation potential was taken in the form proposed by Perdew and Wang [14]. The self-consistent calculations were carried out on a k mesh of 1210 k points in each direction of the Brillouin zone. The calculations were performed fully relativistically including the relativistic effect of the spin-orbit coupling for the values of lattice parameters listed in Table 1. The spin-orbit calculations with both perturbation and fully relativistic approach gives similar results. All data presented in figures comes from the elk code (perturbative approach to SOI).

The structural optimization calculations were performed by the QE-package using ultrasoft pseudopotentials [16,17] with kinetic energy and charge density cut-off of 50 Ry and 500 Ry, respectively, and the $16 \times 16 \times 16$ k point mesh. For structural optimization both LDA [15] and GGA [13] were used, since it is well known that the former approximation underestimates the lattice constant and cohesive energies and the latter one overestimates these parameters. Experimental structural data for $CaIrSi_3$ were used as initial parameters to obtain crystallographic data for $CaPtSi_3$ by the Broyden-Fletcher-Goldfarb-Shanno (BFGS) optimization method [18]. This is justified by the fact that Ir and Pt have similar atomic radii and masses and that their experimental lattice constants differ by less than 0.03 Å and 0.06 Å along the a and c axis, respectively. To our knowledge, experimental data for the atomic positions in $CaPtSi_3$ have not been published yet.

3. Results and discussion

The results of the structure optimization are summarized in Table 1. As expected, the crystallographic data for $CaIrSi_3$ obtained in different approximations are under- (LDA) and over-estimated (GGA), but the mean values are in reasonable agreement with experiment. The differences between the mean values of the LDA

---

* Corresponding author. Tel.: +48 618695125.
E-mail address: jakub_k@ifmpan.poznan.pl (J. Kaczkowski).

0925-8388/$ – see front matter © 2011 Elsevier B.V. All rights reserved.
doi:10.1016/j.jallcom.2011.03.066

Table 1
Lattice parameters, fractional coordinates and interatomic distances of CaIrSi$_3$ and CaPtSi$_3$ from LDA and GGA calculations. Fractional coordinates for tetragonal I4 mm space group are: Ca (0,0,0), Ir or Pt (0,0,z), Si(1) (0,0,z) and Si(2) (0, 0.5,z); only the z parameter is given in the table. In the last column, the arithmetic mean of the data obtained from both LDA and GGA calculations are presented. Experimental data are taken from [6].

Lattice parameters [Å]	Experiment	LDA	GGA	Mean
CaIrSi$_3$				
a	4.18327(2)	4.159	4.214	4.186
c	9.87278(7)	9.779	9.909	9.844
Interatomic distances [Å]				
Ir–Si(1)	2.3396(1)	2.329	2.365	2.347
Ir–Si(2)	2.3674(1)	2.352	2.384	2.368
Si(1)–Si(2)	2.5669(1)	2.542	2.571	2.557
Ca–Si(1)	3.0897(1)	3.074	3.115	3.094
Ca–Si(2)	3.1687(1)	3.141	3.180	3.161
Ca–Ir	3.2931(1)	3.273	3.317	3.295
Fractional coordinate				
Ir	0.64666(15)	0.6469	0.6469	0.6469
Si(1)	0.40975(29)	0.4087	0.4082	0.4085
Si(2)	0.25886(18)	0.2593	0.2595	0.2594
CaPtSi$_3$				
a	4.209	4.200	4.266	4.233
c	9.816	9.751	9.884	9.817
Interatomic distances [Å]				
Pt–Si(1)	–	2.357	2.400	2.379
Pt–Si(2)	–	2.393	2.432	2.412
Si(1)–Si(2)	–	2.507	2.538	2.523
Ca–Si(1)	–	3.126	3.178	3.152
Ca–Si(2)	–	3.149	3.338	3.244
Ca–Pt	–	3.275	3.326	3.300
Fractional coordinate				
Pt	–	0.6444	0.6445	0.6444
Si(1)	–	0.4026	0.4017	0.4022
Si(2)	–	0.2621	0.2626	0.2623

and GGA data and the experimental lattice constants in the case of CaIrSi$_3$ amount to 0.003 Å and −0.029 Å for a and c lattice parameters, respectively. The corresponding differences in the case of the interatomic distances take values from −0.01 Å (Si(1)–Si(2)) to less than 0.001 Å (Ir–Si(2)). Similarly, the mean lattice constants of CaPtSi$_3$ obtained in the same way are in agreement with experimental data (differences amount to 0.024 Å and 0.001 Å for the a and c lattice parameters, respectively) [6]. The calculated interatomic distances for CaPtSi$_3$ need an experimental verification. Those mean parameters represented the starting point for the calculations of the electronic structure of CaPtSi$_3$. Figs. 1 and 2 show the electronic density of states (DOS) for both systems near the Fermi level obtained by the elk-1.0.0 code. In Fig. 1, the total density of states with and without spin–orbit interaction (SOI) is shown. Near the Fermi energy (E_F), there are no visible differences in the range of −0.1 to 0.2 Ha in either compound. The main difference appears between −0.25 Ha and −0.23 Ha and is related to the splitting of the Ir/Pt d states due to the SOI. The Ir d states lie slightly closer to the Fermi level than the Pt d states. The values of the total DOS with (without) SOI at E_F are N(E_F) = 1.81 (1.80) states/eV for CaIrSi$_3$ and 1.43 (1.43) states/eV for CaPtSi$_3$. From the full-relativistic FPLO calculations these values amount to 1.93 and 1.38 states/eV, respectively. It can be compared with the same quantity for BaPtSi$_3$: 1.64 (1.60) states/eV [4]. On the basis of the Sommerfeld expansion one can calculate the coefficient γ determining the electronic contribution to the specific heat. Its values are γ = 4.3 (4.6) mJ/(mol K^2) for CaIrSi$_3$ and 3.4 (3.3) mJ/(mol K^2) for CaPtSi$_3$ (in the parentheses the data obtained from full-relativistic calculations are given), which are also comparable to those for BaPtSi$_3$ (3.8 mJ/(mol K^2) [4]). This is caused by the fact that in all these compounds the main contribution to DOS at E_F comes from the Si p-states (see Fig. 2). However, for CaIrSi$_3$ the contribution from the Ir d-states is also significant, which is reflected in the higher value of N(E_F) as well as in the specific heat coefficient. Due to the fact that the masses of the Ir and Pt atoms do not differ much, according to the BCS theory the higher value of N(E_F) is responsible for a higher T_c in CaIrSi$_3$. The contributions from the Pt d states in CaPtSi$_3$ are lower. The contributions from the Ca p states in CaIrSi$_3$ are almost negligible. Our results are in a reasonable agreement with the experimental data: γ = 5.8 mJ/(mol K^2) and 4.0 mJ/(mol K^2) [6] for the normal state. In Figs. 3 and 4, the band structures are presented for both compounds. The bands near the Fermi energy are split into two groups due to the spin–orbit interaction, the values of this splitting at the Γ-point amount to 0.37 eV for CaIrSi$_3$ and 0.25 eV for CaPtSi$_3$. These values are lower than that for BaPtSi$_3$ (∼0.5 eV) [4]. In CaIrSi$_3$ there are three sets of bands crossing the Fermi level: one set in the directions Γ–X, Γ–P and Γ–N (Fig. 3a) and the other two in the direction Σ–Γ (Fig. 3b). On the other hand, for CaPtSi$_3$ there are two such sets: one crossing the Fermi level in the same way as for CaIrSi$_3$ and the second one crossing it in the Γ–P and Γ–N directions. A similar situation appears in BaPtSi$_3$. Yet, another similarity to BaPtSi$_3$ is that in neither compound the bands cross the Fermi level in the Γ–Z direction. The splitting of the bands crossing the Fermi level is small. Again, similarly as in BaPtSi$_3$, visible splitting appears in the Γ–P and Γ–N directions. Those similarities and differences are reflected in rather complex structures of the Fermi surface of the investigated

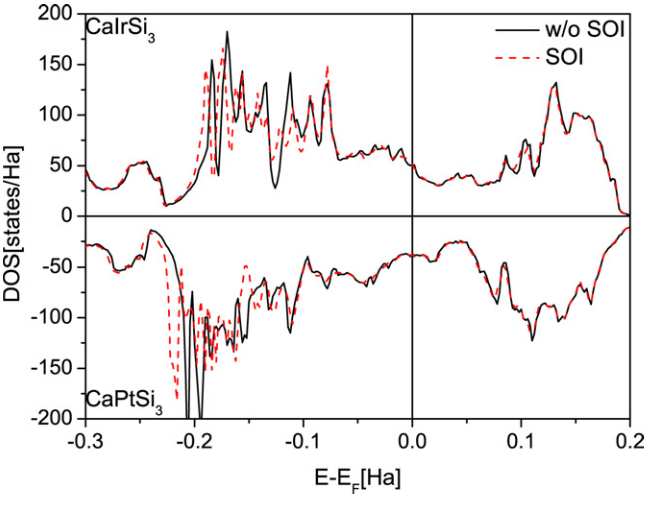

Fig. 1. Total density of states for CaIrSi$_3$ (upper panel) and CaPtSi$_3$ with (dashed line) and without (solid line) spin-orbit interaction (SOI).

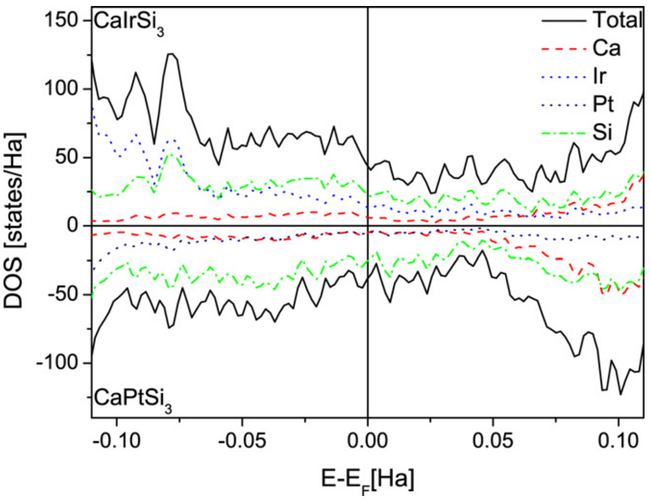

Fig. 2. Total and projected density of states for CaIrSi$_3$ (upper panel) and CaPtSi$_3$.

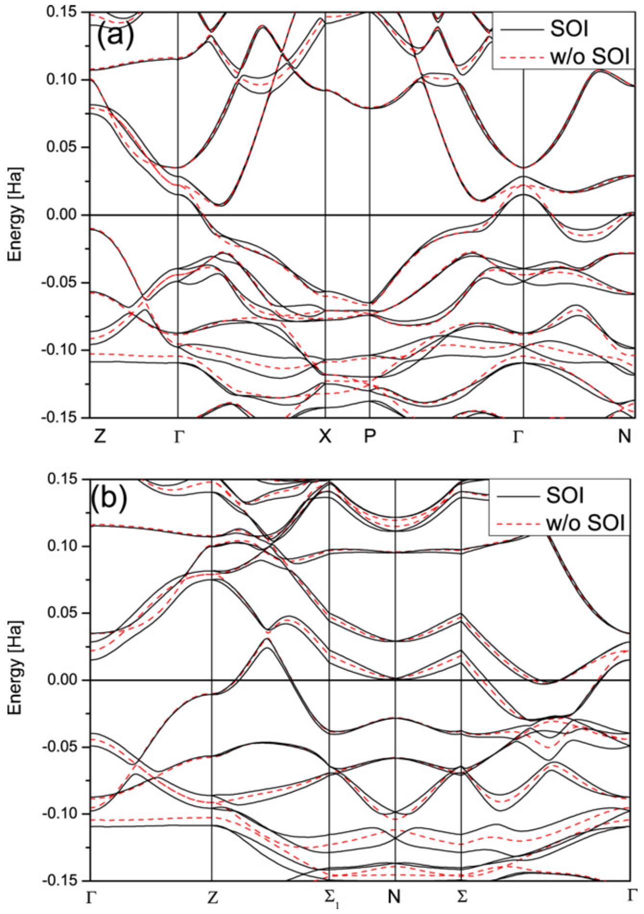

Fig. 3. Band structure of CaIrSi$_3$ with (solid line) and without (dashed line) spin–orbit interaction for the experimental crystallographic structure.

compounds (see Figs. 5 and 6). The Fermi surface of CaPtSi$_3$ is very similar to that of BaPtSi$_3$. The first set of bands crosses the Fermi level in a similar way in both compounds, so the shape of Fermi surface is also very similar for both the systems investigated and for BaPtSi$_3$. The second set of bands do not cross the Fermi surface in CaIrSi$_3$ as it does in CaPtSi$_3$, hence the shape of these bands differ much more. Finally, the third set exceeds slightly the Fermi level only in CaIrSi$_3$ at the point between Σ–Γ direction (see band structure in Fig. 3b), which is visualized in Fig. 5. Due to the small band splitting, the bands in the sets are very similar to each other. The same fact is also responsible for the similar BCS-like behavior of the compounds in question [6].

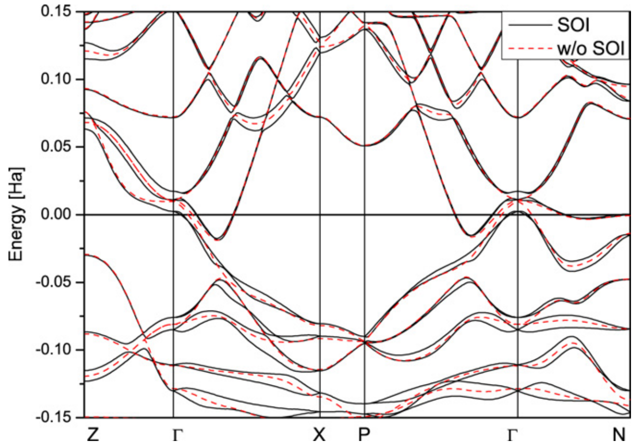

Fig. 4. Band structure of CaPtSi$_3$ with (solid line) and without (dashed line) spin–orbit interaction for the mean lattice parameter from LDA and GGA calculations.

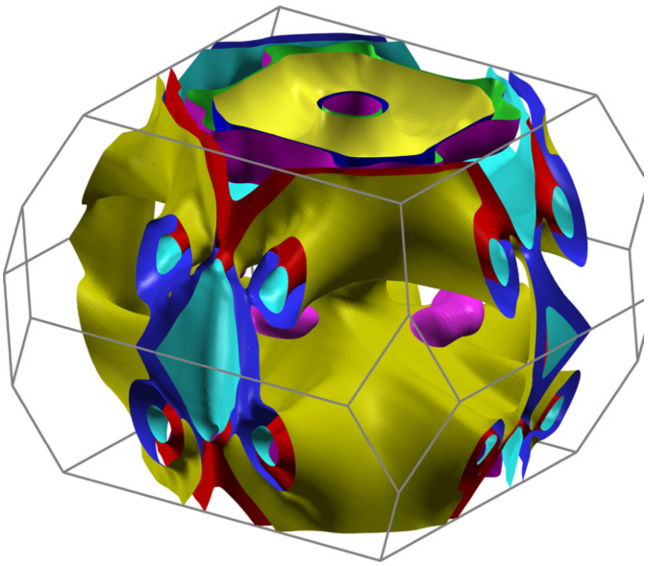

Fig. 5. Overall view of the Fermi surface for CaIrSi$_3$.

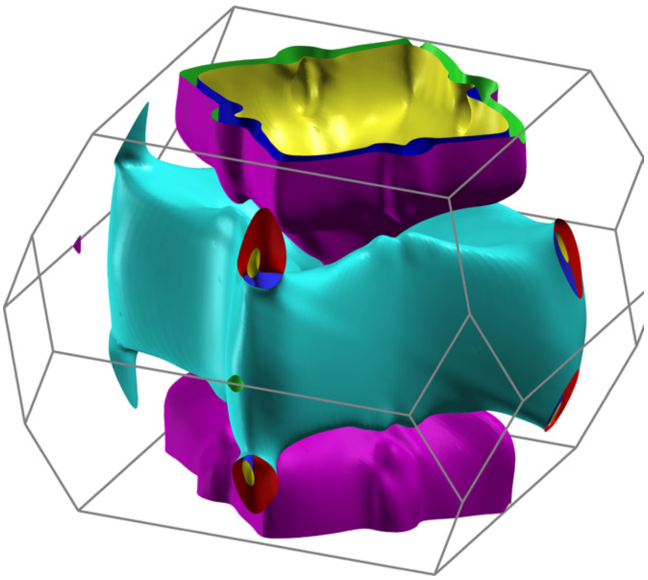

Fig. 6. The Fermi surface for CaPtSi$_3$.

4. Conclusion

To conclude, we have presented the calculations within the density functional approach of the electronic and structural properties of two newly discovered noncentrosymmetric superconductors CaIrSi$_3$ and CaPtSi$_3$. For the first compound, the calculations were made with the use of the experimental crystallographic data, for the second one the crystallographic data were computed on the basis of the structural optimization method relying on the data for the first compound. In the latter case, the mean structural parameters obtained from both LDA and GGA functionals are in a very good agreement with the experimental ones for CaIrSi$_3$. The electronic structures of both compounds show similarities to that of the BaPtSi$_3$ discovered earlier [4] and this could explain the fact that all of them behave in a very similar way [6]. During revision of the paper we learned that crystallographic data for CaPtSi3 have been published in updated version of [6]. Our theoretical predictions are in reasonable agreement with the experimental measurements.

References

[1] L.P. Gor'kov, E.I. Rashba, Phys. Rev. Lett. 87 (2001) 037004.

[2] E. Bauer, G. Hilscher, H. Michor, Ch. Paul, E.W. Scheidt, A. Gribanov, Yu. Seropegin, H. Noël, M. Sigrist, P. Rogl, Phys. Rev. Lett. 92 (2004) 027003.

[3] Ch. Pfleiderer, Rev. Mod. Phys. 81 (2009) 1551–1624.

[4] E. Bauer, R.T. Khan, H. Michor, E. Royanian, A. Grytsiv, N. Melnychenko-Koblyuk, P. Rogl, D. Reith, R. Podloucky, E.-W. Scheidt, W. Wolf, M. Marsman, Phys. Rev. B 80 (2009) 064504.

[5] G. Eguchi, D.C. Peets, M. Kriener, S. Maki, E. Nishibori, H. Sawa, Y. Maeno, Physica C 470 (2010) S762.

[6] G. Eguchi, D.C. Peets, M. Kriener, Y. Maeno, E. Nishibori, Y. Kumazawa, K. Banno, S. Maki, H. Sawa, Phys. Rev. B 83 (2011) 024512.

[7] H. Eschrig, The Fundaments of Density Functional Theory, 2nd ed., Edition am. Gutenbergplatz, Leipzig, 2003.

[8] http://elk.sourceforge.net/.

[9] P. Giannozzi, et al., J. Phys.: Condens. Matter 21 (2009) 395502.

[10] http://www.quantum-espresso.org.

[11] K. Koepernik, H. Eschrig, Phys. Rev. B 59 (1999) 1743–1757.

[12] H. Eschrig, M. Richter, I. Opahle, in: P. Schwerdtfeger (Ed.), Relativistic Solid States Calculations, Relativistic Electronic Structure Theory, Part 2. Applications, Elsevier, New York, 2004, pp. 723–776.

[13] J.P. Perdew, K. Burke, M. Ernzerhof, Phys. Rev. Lett. 77 (1996) 3865–3868.

[14] J.P. Perdew, Y. Wang, Phys. Rev. B 45 (1992) 13244–13249.

[15] J.P. Perdew, A. Zunger, Phys. Rev. B 23 (1981) 5048–5079.

[16] D. Vanderbilt, Phys. Rev. B 41 (1990) 7892–7895.

[17] D. Vanderbilt, http://www.physics.rutgers.edu/~dhv/uspp/.

[18] B.G. Pfrommer, M. Côté, S.G. Louie, M.L. Cohen, J. Comput. Phys. 131 (1997) 233–240.